IEEE Access
Multidisciplinary | Rapid Review | Open Access Journal

Received July 9, 2019, accepted July 29, 2019, date of publication August 12, 2019, date of current version August 29, 2019.

Digital Object Identifier 10.1109/ACCESS.2019.2934820

Proposal of a Fuzzy Controller for Radial Position in a Bearingless Induction Motor

EVANDRO AILSON DE FREITAS NUNES[1], ANDRÉS ORTIZ SALAZAR[1], (Member, IEEE), ELMER ROLANDO LLANOS VILLARREAL[2], (Member, IEEE), FRANCISCO ELVIS CARVALHO SOUZA[3], LUCIANO PEREIRA DOS SANTOS JÚNIOR[3], JOSÉ SOARES BATISTA LOPES[3], AND JUAN CARLOS CUTIPA LUQUE[4], (Member, IEEE)

[1]Department of Computer Engineering and Automation, Federal University of Rio Grande do Norte, Natal 59072-970, Brazil
[2]Department of Natural Sciences, Mathematics and Statistics, Federal Rural University of Semi-arid, Mossoró 59625900, Brazil
[3]Federal Institute of Education, Science and Technology of Rio Grande do Norte, Natal, Brazil
[4]Department of Electronics Engineering, Universidad Nacional de San Agustin de Arequipa, Arequipa 04001, Peru

Corresponding author: Elmer Rolando Llanos Villarreal (elmerllanos@ufersa.edu.br)

This work was suported in part by the Comissão de Aperfeiçoamento de Pessoal do Nível Superior (CAPES), in part by the Conselho Nacional de Desenvolvimento Científico e Tecnológico (CNPq), and in part by the UNSA Investiga under Grant IAI-019-2018-UNSA.

ABSTRACT In this paper, a radial position control approach of a bearingless induction motor is proposed. The rotor is supported by magnetic forces, which is complex to model. Generally, simplifications are adopted to determine a linearized model that hinders classical controllers' performance. On the other hand, fuzzy controllers have non-linear characteristics and do not require precise mathematical models. Instead, it uses the experience and knowledge of human operators to build a knowledge base to be used on the control. The prototype under study is a three-phase induction motor without a rated power of 1 HP, 4-pole, 220/380V and rated current 3/1.75A. It operates on a vertical axis, so there is no need to compensate for the rotor weight. The paper proposes the implementation of a Mamdani Fuzzy PD controller in order to control the rotor radial position of a three-phase induction motor by means of a Texas Instruments TMS320F28335 Digital Signal Processor (DSP). We present experimental results that validate the good performance of the fuzzy controller.

INDEX TERMS Fuzzy controller, DSP, bearingless induction motor, split windings machine.

I. INTRODUCTION

There are several applications involving electric machines wherein maintenance becomes a challenge due to the working conditions of them, e.g., motors under great depths, high temperatures, or in impermeable environments [1]. One of the engine components that require a lot of maintenance is the mechanical bearings, due to the natural wear and tear. This fact led researchers in the 1970s to study the magnetic suspension applied to rotorless non-contact rotor systems, the so-called magnetic bearings [2]. This device solves the wear problem of the mechanical bearings but increases the size of the machine [3]–[6]. A solution to overcome the drawbacks of magnetic machines are the bearingless machines that avail their own windings to produce magnetic forces that keep the machine rotor centralized. These bearings, as well as magnetic bearings, do not require lubrication, have a no-noise operation and are suitable for applications with an unusual rotational speed (above 3600 rpm) [7].

There are basically two structures for bearingless induction machines: two winding systems and split winding systems. The first one was proposed by [8] and consists of adding an extra set of windings that enables flux distribution changing through the magnetic overlap to produce radial positioning forces, and torque aiming mechanical rotation. The second one proposed in [9] spatially divides the stator windings into coil groups that are responsible for regulating flux distributions through the current imbalance among them. The first work with this type of system employed a biphasic four-pole motor, in which the winding of one of the phases is divided into four groups arranged symmetrically and orthogonally to each other [10].

Then, it was proposed the implementation of a three-phase motor with four poles, wherein each phase is divided into pairs of opposing groups, for a total of six coils in the stator [11]. The mentioned proposal had its successful

The associate editor coordinating the review of this article and approving it for publication was Jinpeng Yu.

implementation and became object of several other studies that explored all the classical techniques (PID) to control the rotor radial position [1], [7], [12], [13] and [14]. In [15], Chiba *et al.* employ PID controllers to regulate the radial position of a bearingless induction motor. However, when the radial electromagnetic force follows the radial force reference signals a phase delay generates a coupling between the so-called alpha-beta axes. As a solution, the authors implemented lead-lag compensators that maintain an average change of 50 um in radial position. This solution makes the strategy implementation more complex and highly sensitive to parametric variations.

In [16], Rodriguez and Santisteban also employ a PID control in radial position regulation and emphasize the need for identifying motor electrical parameters for a good controllers' performance. In the experimental results, the authors realize that the median values on the y-axis reach almost 10 times the median values observed in the x-axis and suggest an automatic angular correction for the y-axis that acts directly on the reference signals of the radial position controllers. However, these controllers are tuned to a certain operating point, and if it suffers a considerable variation, the controller decreases performance or even stability margin. In addition, electric machines are nonlinear systems with parameters susceptible to uncertainties that may hamper the performance of classical controllers. Furthermore, due to the current difficulty in modeling suspension forces, many simplifications are required to determine a representative linear model [1], [7], [17].

In order to overcome classical PID limitations, several other strategies have been proposed like genetic-algorithms [18]–[27] and artificial intelligence [28], [29], with special attention given to a fuzzy controller [18].

Fuzzy systems allow the analysis of a problem from a humanlike point of view by using linguistic variables. It also allows for a gradual transition between sets. Thus, fuzzy control systems can be modeled to emulate strategies that humans use to solve problems, and due to this feature is considered an intelligent system. These systems provide a formal method of translating verbal, vague, imprecise, and qualitative expressions, usual in human communication, into numerical values [18]. The basic structure of a rule-based fuzzy controller consists of three steps: Fuzzification, Inference, and defuzzification. In fuzzification, the input data are coded or converted into fuzzy values, that is, qualitative or linguistic values understandable by the inference mechanism.

The fuzzification process occurs through the application of membership functions in the input variables. The inference is responsible for the application of rules and fuzzy operations in order to map input linguistic values to output linguistic values. In defuzzification, fuzzy values resulting from inference are converted into crisp values, that is, numerical quantities by means of membership functions in the output variable [19].

With these considerations, it is proposed the application of a controller based on fuzzy logic in order to keep a machine rotor centralized even if lacking some variable specifications.

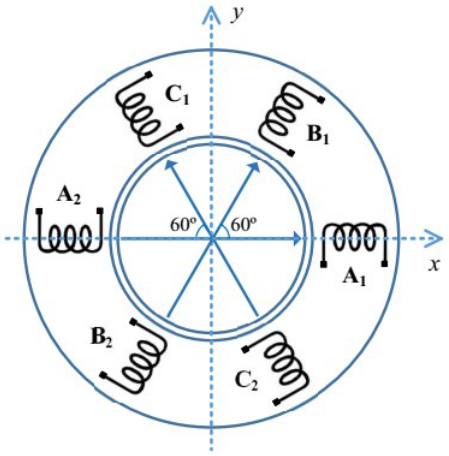

FIGURE 1. Stator winding arrangement.

This type of controller has non-linear characteristics and does not require precise mathematical models. Instead, it uses the experience and knowledge of human operators to build a knowledge base necessary for control [18]. Diffuse logic proved to be a powerful and effective tool in motor drive and control applications [20]–[23]. However, applications in magnetic suspension systems, especially in bearingless motors, are incipient. In [24], He *et al.* present an adaptive fuzzy PID controller to control the radial rotor position of a non-rolling switched reluctance motor. In the case of bearingless induction motors [25], the fuzzy control is applied to the angular speed loop, but no fuzzy control applications were found in the radial positioning of the rotor of these machines. The purpose of this paper is to implement a fuzzy PD controller to regulate the rotor radial position of a three-phase induction machine with split windings embedded in a Texas Instruments TMS320F28335 Digital Signal Processor (DSP).

The next sections of this paper will be organized as follows: in section II is presented the preliminary concepts. In section III is presented the system description. In section IV is presented the control strategy. In section V is presented the fuzzy controller. In section VI is presented the experimental results. Finally, in section VII are presented the conclusions of this paper.

II. PRELIMINARY CONCEPTS

A. OBTAINING RADIAL FORCES

To understand the configuration of radial forces acting on the rotor, it is necessary to visualize the internal distribution of the magnetic flux and the arrangement of the windings within the stator from a cross-section of the machine depicted in Fig. 1.

The magnetic flux configuration due to feeding A_1 and A_2 coils is depicted in Fig. 2. Feeding these coils with the same electric current results in a magnetic flux configuration represented in the left side of Fig. 2. Assuming the rotor is in the center of the stator, the magnetic flux density in both sides along the x-axis are equal, so there is no resulting horizontal force acting on the rotor.

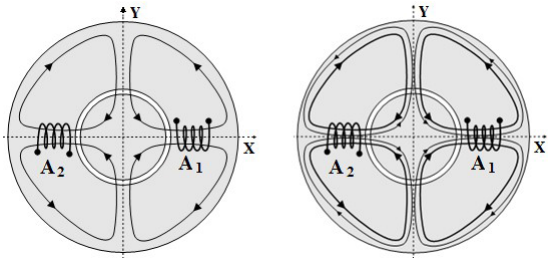

FIGURE 2. Configuration of the magnetic flux produced by coils A_1 and A_2. Additional magnetic flux caused by the differential variation of the currents of A_1 and A_2 (right).

By increasing the current value, Δi_a in the winding A_1 and simultaneously decreasing the same value in the flux of the winding A_2, an additional magnetic flow arises as shown in the right side of Fig. 2 through the thinner lines. This additional flux joins the flux of A_1 and opposes the flux of A_2, originating magnetic flux imbalance which generates a radial magnetic force on the rotor in the positive direction of $x-$axis. Through this differential action on the currents flowing through the two remaining coils, the forces are generated and modify the rotor position. This is valid for any pair of opposing coils, and the force obtained acts along the axis passing through the center [7]. In this way, the positioning forces are controlled in any transverse plane direction, overlapping the effects along the three actuation axes, as shown in Fig. 1, by the arrows drawn inside the rotor.

III. SYSTEM DESCRIPTION

The prototype under study is a 1HP, fourpoles, 220/380V and nominal current 3/1.75A three-phase induction motor. The motor shaft is orthogonally positioned in relation to the prototype base in order to mitigate the rotor weight effects. Both the rotor and the stator have undergone changes in their structure, as described below, and these modifications do not disfigure the induction machine configuration.

A. ROTOR CONFIGURATION

The traditional squirrel cage rotor does not present a satisfactory response to the radial positioning control, due to the appearance of induced currents with the same stator frequency content in the rotor. The existence of bipolar flux control components in the rotor is not desirable, because they would cause a delay in the response of the controller [17]. This problem is overcome by employing a four-pole winding rotor. This configuration ensures that only four-pole fields belonging to the feed frequency of the machine are induced. It prevents bipolar magnetic fluxes from being generated due to the modulated control components in the stator currents [7] and [17].

B. STATOR CONFIGURATION

The stator winding consists of six groups of coils, two per phase. Fig. 3 shows how the six groups are connected to start

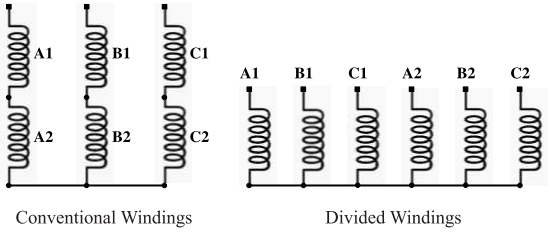

FIGURE 3. Difference between conventional and divided winding.

the engine. In that sense, the only difference compared to a conventional motor is that the pairs of opposing groups are not connected in series. Instead, they are divided into pairs, making it possible to feed each of them independently.

The feeder currents should produce the required torque and generate restoring forces to regulate the rotor radial position. Thus, the stator currents are divided into the three-phase reference currents I_a, I_b and I_c responsible for the torque, and the positioning components Δi_a, Δi_b and Δi_c are calculated by the position controllers. Therefore, the currents of the six groups of windings are determined by equation (1).

$$\begin{aligned} I_{a1} &= I_a + \Delta i_a \\ I_{a2} &= I_a - \Delta i_a \\ I_{b1} &= I_b + \Delta i_b \\ I_{b2} &= I_b - \Delta i_b \\ I_{c1} &= I_c + \Delta i_c \\ I_{c2} &= I_c - \Delta i_c \end{aligned} \tag{1}$$

C. ACTIVATION

The developed bearingless motor drive structure is depicted in Fig. 4. It consists of two-stage conversion. The first one employs a non-controlled diode-based rectifier responsible for delivering energy to dc-link electrolytic capacitors. The second stage performs DC-AC conversion by means of two three-phase Voltage Source Inverters (VSIs). Each of the six arms employs an IGBT SEMIKRON module and is responsible for feeding the motor bearing coils individually.

IV. CONTROL STRATEGY

The block diagram of Fig. 5 shows the system control strategy scheme. It consists of two control loops. The first one is responsible for regulating the stator currents and the second one is responsible for regulating the rotor radial position. The speed regulation is performed by an open loop strategy.

A. POSITION CONTROL

The control strategy is depicted in Fig.5; wherein two orthogonally positioned sensors acquire xy axes radial position signals. These signals are compared to the position references, and position error signals Δi_x and Δi_y, respectively, and then converted to the stationary reference frame by means of Clark transform ($2\phi/3\phi$ block). The imbalance of the currents is

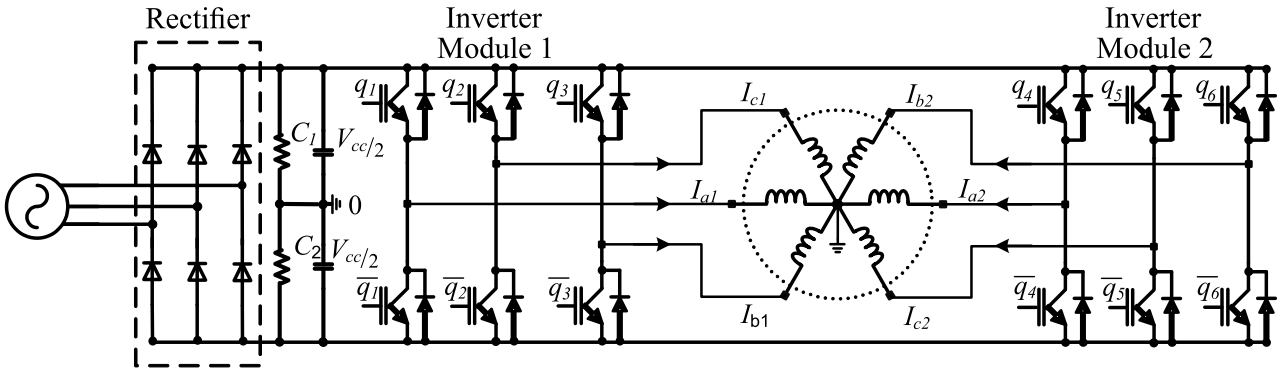

FIGURE 4. Drive structure of the bearingless motor.

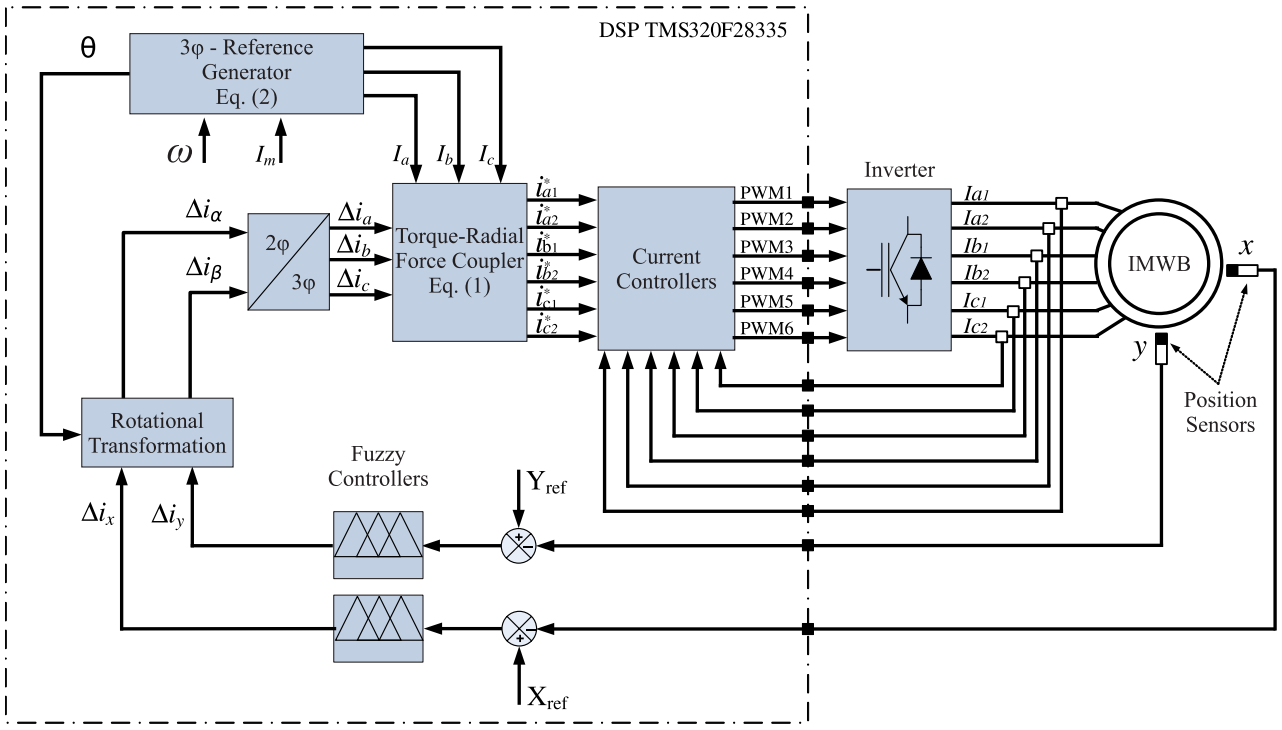

FIGURE 5. Block diagram of the control system.

performed by applying equation (1), resulting in six reference values for the stator current controllers.

B. CURRENT CONTROL

Current control is performed by six identical and independent proportional-integral (PI) digital controllers, one for each stator coil. These controllers compare current references produced by equation (1) with the currents read directly from the current sensors and thus generate the control signals to be applied to the coils through the VSIs. The three-phase reference currents are digitally generated in DSP by:

$$\begin{aligned} I_a &= I_m sin(\omega t) \\ I_b &= I_m sin(\omega t - \frac{2\pi}{3}) \\ I_c &= I_m sin(\omega t + \frac{2\pi}{3}) \end{aligned} \tag{2}$$

wherein ω is the angular frequency and I_m maximum current amplitude. The current controller design can be found in [7], however the tuning was performed empirically.

V. FUZZY CONTROLLER

According to [9]–[14], the radial position model of a split winding bearingless three-phase machine is open-loop unstable due to a right half-plane pole for each direction axis. This pole existence hampers a PD strategy implementation that adds a zero on the left half-plane to ensure that the feedback loop is stable. In addition, system tuning becomes more complex and highly sensitive to parametric variations. In this work, a fuzzy controller with traditional PD features and able to deal with model imperfections replaces the controller adopted in [9]. In order to control the radial position of the rotor, two independent fuzzy PD controllers of the Mamdani

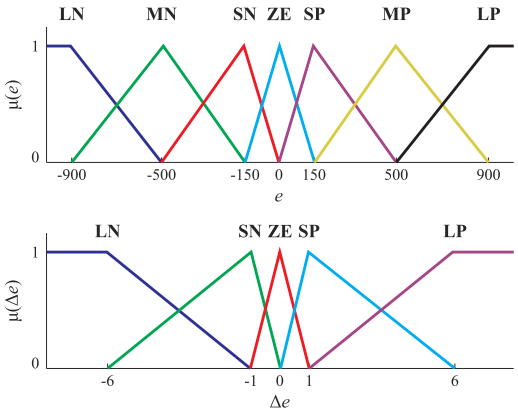

FIGURE 6. Membership functions of input variables.

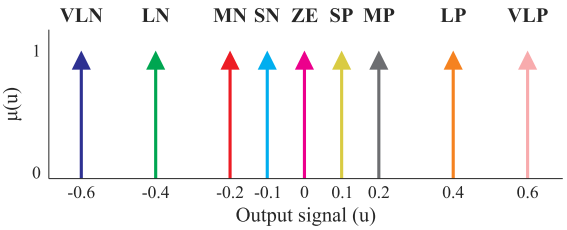

FIGURE 7. Membership functions of output variables.

type were implemented, one for the x-axis and one for the y-axis, according to the diagram in Fig. 5.

The basic structure of a rules-based fuzzy controller consists of three stages: fuzzification, inference and defuzzification [18]. In the fuzzification, input data are converted into fuzzy values, i.e., qualitative values comprehensible by the inference mechanism.

A. MEMBERSHIP FUNCTIONS

For each controller, five triangular and two rectangular membership functions were defined for the error variable and three triangular and two rectangular membership functions for the change in the error variable, according to Fig. 6. For generating the output, nine singleton functions were chosen, as depicted in Fig. 7. With these functions, the defuzzification is done simply by the formula:

$$\Delta_i = \frac{\sum_{i=1}^{N} u_i \sum_{i=1}^{N} \mu_{out}(u_i)}{\sum_{i=1}^{N} \sum_{i=1}^{N} \mu_{out}(u_i)} \tag{3}$$

wherein u_i is the i^{th} membership function, $\mu_{out}(u_i)$ represents its degree of membership and N the number of employed functions [18].

Through experiments with the machine, we defined the speech universes of the input and output variables [26]. Otherwise, it determined the range from -1500 to 1500, for a range variation of -10 to $+10$. (These numbers are not in physical units, they are called directly from the A/D of the DSP).

With respect to the output variable Δ_i (control signal), the speech universe was defined based on previous knowledge obtained from previous experiments with another controller [14]. Thus, the proposed speech universe Δ_i was the range of -0.6 to $+0.6$.

TABLE 1. Linguistic labels adopted to describe fuzzy sets.

Label	Signification
VLN	Very Large Negative
LN	Large Negative
MN	Medium Negative
SN	Small Negative
ZE	Zero
SP	Small Positive
MP	Medium Positive
LP	Large Positive
VLP	Very Large Positive

Initially, membership functions were distributed evenly in the speech universe. Afterward, adjustments were performed experimentally by changing functions closer to the zero function to achieve higher precision and better performance of the controllers. They were used as membership functions in both axes.

B. RULES BASIS

Defining the rule sets is directly related to the aim of the control. Since the bearingless motor aims to keep the rotor centralized, the main task is to minimize the position tracking error. The higher the error, the higher the control input. However, a change in error also affects the value of the control input. Consequently, the error and change in error are used in the control rules as the linguistic variables. These are defined as:

$$\begin{aligned} e &= error = P_{ref} - P_{meas} \\ \Delta_e &= change\ in\ error = e[k] - e[k-1] \end{aligned} \tag{4}$$

wherein e is the error signal, P_{ref} is the position reference, P_{meas} is the axis position measured by the acquisition device, $e[k]$ is the actual error and $e[k-1]$ the error calculated in the previous sample of k.

The rules of fuzzy controller are of the form:

$$\begin{aligned} &If\ error\ = A\ and\ change\ in\ error = B \\ &Then\ u = C \end{aligned} \tag{5}$$

The memberships functions are named by linguistic labels that are summarized in Table (1). The rule base is summarized into a table in which the columns represent the error variable and the lines represent the change in error. The x-axis rand y-axis rule bases are summarized in Table (2) and Table (3), respectively. The a, b, c and d mean Δ_{e_x}, e_x, Δ_{e_y} and e_y, respectively.

An initial rule base was developed using prior knowledge of the system. Then adjustments were made based on the behavior of the system during the experiments. The rules were changed until they could no longer improve the response, so the membership functions were adjusted. The adjustments of the rules were intercalated with the adjustments of the membership functions, never both at the

TABLE 2. Rules for *x*-axis fuzzy controller.

a \ b	LN	MN	SN	ZE	SP	MP	LP
LP	VLN	VLN	VLN	VLN	LN	SN	SN
SP	VLN	LN	MN	ZE	SP	LP	LP
ZE	LN	SN	SN	SP	MP	LP	VLP
SN	VLN	LN	MN	ZE	SP	LP	LP
LN	SP	LP	LP	LP	SP	VLP	VLP

TABLE 3. Rules for *y*-axis fuzzy controller.

c \ d	LN	MN	LN	ZE	SP	MP	LP
LP	VLN	VLN	VLN	LN	MN	MN	SN
SP	VLN	MN	MN	MN	ZE	SP	SP
ZE	LN	MN	ZE	ZE	SP	MP	LP
SN	SN	SN	SP	SP	MP	LP	VLP
LN	SP	MP	LP	LP	LP	VLP	VLP

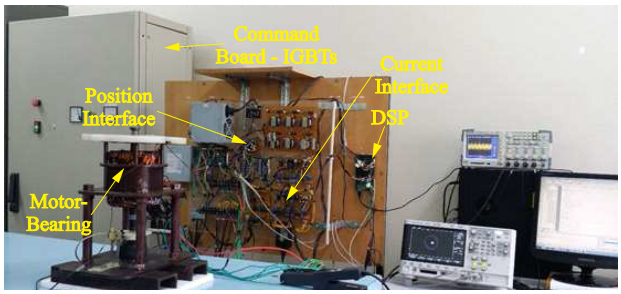

FIGURE 8. Experimental setup of the system.

same time. The adjustments originated the error and change in error membership functions illustrated in Fig. 6 and the output membership functions depicted in Fig. 7 and the rules summarized in Table (2).

VI. EXPERIMENTAL RESULTS

The experimental setup of the bearingless motor control is depicted in Fig. 8 according to the Fig. 4. The control is performed by Texas instruments DSP TMS320F28335, incorporated into the Spectrum Digital $eZdsp^{TM}$ kit. The period adopted for sampling the signals is $100\mu s$ in order to reduce switching losses and improve the prototype efficiency [30].

In order to verify the performance of the controller, experimental tests were carried out. The stator cross-section center corresponding to the coordinate system point (x,y)=(0,0) was adopted as the reference radial position. It is the position that the rotor must operate. Fig. 9 shows the steady-state behavior of the system, when the rotor speed reaches 1774 rpm and oscillates around the reference position with an average error of -0.000206mm (0.052%) and -0.000743mm (0.186%) in the x and y directions, respectively. The dynamics of the two axes is slightly different, so there is also a low-frequency oscillation on the *y*-axis.

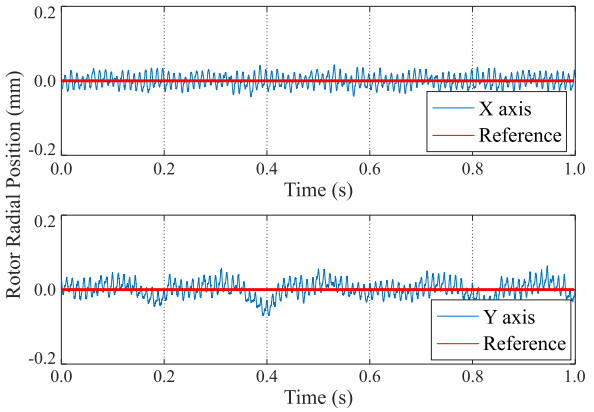

FIGURE 9. Radial position at steady state.

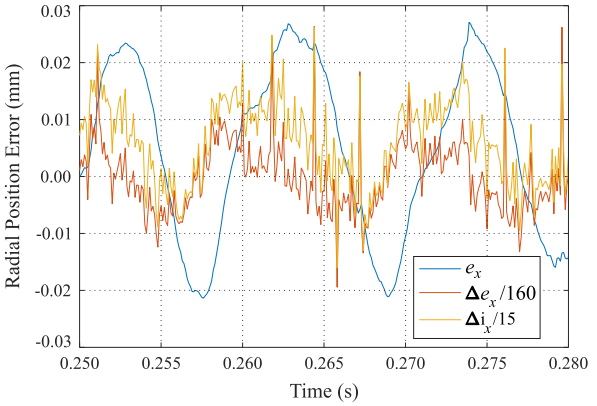

FIGURE 10. Position error, change in error and control signal on *x*-axis.

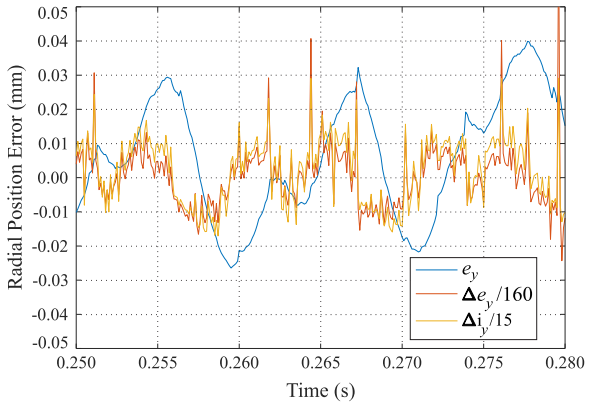

FIGURE 11. Position error, change in error and control signal on *y*-axis.

The amplitude of the rotor oscillation around the reference can be seen in Fig. 10 and Fig. 11. These figures show the position error (which coincides with the position, since the reference is zero) to the error variation and the control signals Δi_x and Δi_y of both controllers (x and y axes). The scale of the error variations was reduced by a factor of 160 when scaling the control signals by a factor of 15, so that they can be visualized along with the error signal.

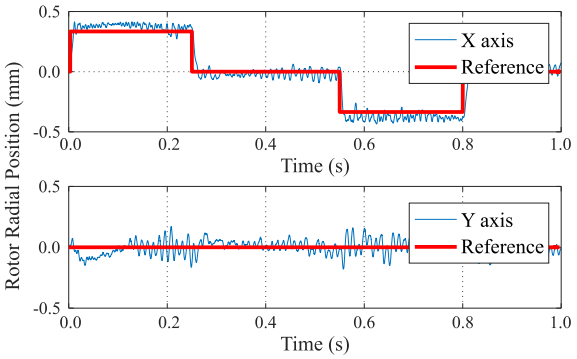

FIGURE 12. System behavior under step disturbance applied on *x*-axis.

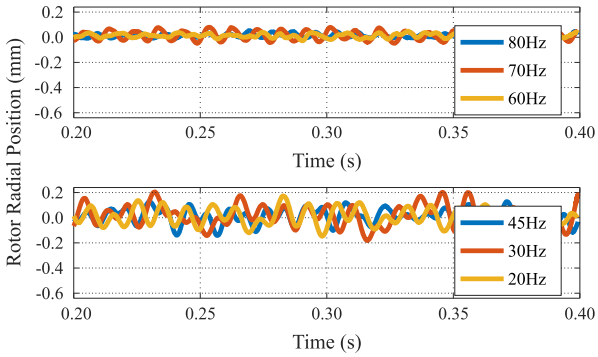

FIGURE 13. Controller response at different frequencies (*x*-axis).

It is observed in Fig. 10 and Fig. 11 that the control signal is proportional to the change in error. It is expected behavior in controllers equipped with derivative gain necessary to stabilize unstable systems as well as the proposed system. Also, it can be seen that there are error variations peaks that are responsible for control spikes. This behavior is due to the roughness on the disk used to measure the radial position.

A slight difference between *xy* axes signals is evident. It occurs due to the radial position reference adopted in this paper, depicted in Fig. 1. The regulation in *x*-axis is performed by phase A and contributions from phase B and C through its coils. On the other hand, there is a decoupling between the x and y reference axis due to the orthogonality between them. So the regulation in the *y*-axis is only performed by the contribution of phases B and C. As a consequence, there is less magnetic flux able to produce magnetic force and regulate the *y*-axis position. This behavior is observed in the error and change in error signals. This leads to larger control signals produced by this position controller.

The controller response to reference value step changes which magnitude varies between $\pm 0.33mm$ is depicted in Fig. 12. The rotor position, when the reference is at $x = 0$, shows a mean error of less than $0.022mm$. Facing the applied steps (0.33 and -0.33) the mean error is $0.047mm$. The existence of a steady-state error is acceptable since the controller is a fuzzy PD [18]. The reference steps were applied only on the *x*-axis, but similar results were also observed when applied on the *y*-axis. The disturbance observed on the *y*-axis is due to a coupling between the axes, caused mainly by the gyroscope effect. Thus, when there are changes of references in the *x*-axis, the *y*-axis is disturbed.

The fuzzy controller is set to operate at a frequency of $60Hz$. However, in order to verify its robustness, the motor is excited with other frequencies, and the results are depicted in Fig. 13. It was verified that it maintains the same performance for frequencies above $60Hz$. At frequencies lower than $60Hz$, the system remains stable but shows the increased amplitude of the oscillations. Similar results were observed on the *y*-axis.

The system performance during motor start-up is depicted in Fig. 14. The positions of each axis as a function of time can be observed in Fig. 14(a). It illustrates the movement towards the reference point, including the acceleration until reaching steady-state behavior, in approximately 14 seconds. The upper waveforms describe *x*-axis position behavior, while the

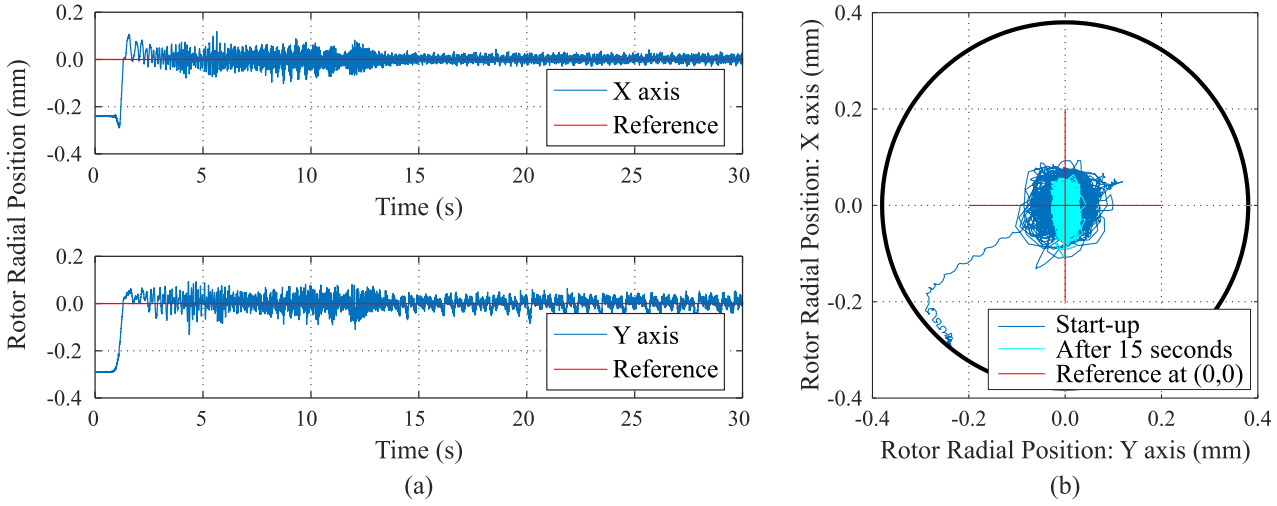

FIGURE 14. System behavior during engine startup for (a) *x* and *y* positions as functions of time and (b) rotor position in the *xy* plane.

lower ones describe *y*-axis position behavior. In Fig. 14(b) the same result is presented in the XY plane, in which the whole behavior is analyzed: rotor displacement for reference, acceleration, and steady-state. The steady-state period is highlighted in the cyano color in the center of Fig. 14(b), we note the small variation of the position on the *x*-axis, and a slightly larger oscillation on the *y*-axis.

VII. CONCLUSIONS

This article aimed to study and implement a fuzzy controller with PD features in the rotor positioning of a bearingless induction motor. The experimental results confirmed the good performance of the implemented fuzzy controller, both at the operating point, as well as at a reference away from it, which shows a certain degree of robustness. The good performance was guaranteed even not knowing the motor nonlinearities and lacking the traditional parameter generally required for tuning classical controllers. Robustness can also be verified with excitation frequencies above 60 Hz. Although performance at the lower frequencies is unsatisfactory, system stability is still maintained. The contribution of this paper is to provide a non-linear control for a system that, depending on the operating conditions, can reveal significant nonlinearities. Previous research has addressed classical control techniques that are limited to systems with linear characteristics. For future work prospects, an optimization of fuzzy controller and new control methods i.e., Neuro-Fuzzy strategies, are planned. In addition, there will be an improvement in the system for disturbance analysis in rotor shaft radial directions, either by an external force or by a torque on the axis.

REFERENCES

[1] J. M. S. Ferreira and A. O. Salazar, "Máquina de indução sem mancais: Modelo e acionamento," *Eletrônica de Potência*, vol. 12, no. 3, pp. 217–222, Nov. 2007.

[2] P. Studer, "A practical magnetic bearing," *IEEE Trans. Magn.*, vol. 13, no. 5, pp. 1155–1157, Sep. 1977.

[3] L. Zhuchong, L. Kun, and Z. Wei, "Inertially stabilized platform for airborne remote sensing using magnetic bearings," *IEEE/ASME Trans. Mechatronics*, vol. 21, no. 1, pp. 288–301, Feb. 2016.

[4] S. Ghiringhelli, F. Braghin, F. Castelli-Dezza, M. S. Carmeli, M. Mauri, and M. Rossi, "New large airgap active magnetic bearings: Modeling and experimental validation," in *Proc. Int. Symp. Power Electron., Elect. Drives, Automat. Motion (SPEEDAM)*, Anacapri, Italy, Jun. 2016, pp. 546–551.

[5] A. Chiba, D. T. Power, and M. A. Rahman, "Characteristics of a bearingless induction motor," *IEEE Trans. Magn.*, vol. 27, no. 6, pp. 5199–5201, Nov. 1991.

[6] A. Chiba, T. Deido, T. Fukao, and M. A. Rahman, "An analysis of bearingless AC motors," *IEEE Trans. Energy Convers.*, vol. 9, no. 1, pp. 61–68, Mar. 1994.

[7] F. E. F. Castro, "Three phase induction bearingless motor with divided winding: Optimization of the radial positioning system," M.S. thesis, UFRN, Natal, Brazil, 2004, p. 105.

[8] A. Chiba, D. T. Power, and M. A. Rahman, "No load characteristics of a bearingless induction motor," in *Proc. IEEE Ind. Appl. Soc. Annu. Meeting*, Dearborn, MI, USA, vol. 1, Sep./Oct. 1991, pp. 126–132.

[9] A. O. Salazar and R. M. Stephan, "A bearingless method for induction machines," *IEEE Trans. Magn.*, vol. 29, no. 6, pp. 2965–2967, Nov. 1993.

[10] A. O. Salazar, R. M. Stephan, and W. Dunford, "An efficient bearingless induction machine," in *Proc. COBEP*, vol. 1, 1993, pp. 419–424.

[11] J. M. S. Ferreira, M. Zucca, A. O. Salazar, and L. Donadio, "Analysis of a bearingless machine with divided windings," *IEEE Trans. Magn.*, vol. 41, no. 10, pp. 3931–3933, Oct. 2005.

[12] V. F. Victor, J. Á. de Paiva, A. O. Salazar, and A. L. Maitelli, "Performance analysis of a neural flux observer for a bearingless induction machine with divided windings," *Revista de Eletrônica de Potência*, vol. 15, pp. 107–114, 2010.

[13] V. F. Victor, F. O. Quintaes, J. S. B. Lopes, L. D. S. Junior, A. S. Lock, and A. O. Salazar, "Analysis and study of a bearingless AC motor type divided winding, based on a conventional squirrel cage induction motor," *IEEE Trans. Magn.*, vol. 48, no. 11, pp. 3571–3574, Nov. 2012.

[14] J. S. B. Lopes, L. P. dos Santos, J. Á. de Paiva, V. F. Victor, A. L. Maitelli, and A. O. Salazar, "Application of neuro-fuzzy estimation for rotor flux in speed vector control of bearingless induction motor," *J. Energy Power Eng.*, vol. 9, pp. 192–198, Apr. 2015.

[15] S. Nomura, A. Chiba, F. Nakamura, K. Ikeda, T. Fukao, and M. A. Rahman, "A radial position control of induction type bearingless motor considering phase delay caused by the rotor squirrel cage," in *Proc. Conf. Rec. Power Convers. Conf.*, Yokohama, Japan, Apr. 1993, pp. 438–443.

[16] E. F. Rodriguez and J. A. Santisteban, "An improved control system for a split winding bearingless induction motor," *IEEE Trans. Ind. Electron.*, vol. 58, no. 8, pp. 3401–3408, Aug. 2011.

[17] A. Chiba, T. Fukao, O. Ichikawa, M. Oshima, M. Takemoto, and D. G. Dorrell, *Magnetic Bearings and Bearingless Drives*, 1st ed. Burlington, VT, USA: Elsevier, 2005.

[18] M. G. Simoes and I. S. Shaw, *Fuzzy Control and Modeling*. 2007.

[19] G. J. Klir and B. Yuan, *Fuzzy Sets and Fuzzy Logic: Theory and Applications*. Upper Saddle River, NJ, USA: Prentice-Hall, 1995.

[20] J. L. P. Azcue and E. Ruppert, "Three-phase induction motor DTC-SVM scheme with self-tuning PI-type fuzzy controller," in *Proc. 7th Int. Conf. Fuzzy Syst. Knowl. Discovery*, Yantai, China, 2010, pp. 757–762.

[21] S. Pati, M. Patnaik, and A. Panda, "Comparative performance analysis of fuzzy PI, PD and PID controllers used in a scalar controlled induction motor drive," in *Proc. Int. Conf. Circuits, Power Comput. Technol. (ICCPCT)*, Nagercoil, India, Mar. 2014, pp. 910–915.

[22] S. Gdaim, A. Mtibaa, and M. F. Mimouni, "Design and experimental implementation of DTC of an induction machine based on fuzzy logic control on FPGA," *IEEE Trans. Fuzzy Syst.*, vol. 23, no. 3, pp. 644–655, Jun. 2015.

[23] H. Sudheer, S. Kodad, and B. Sarvesh, "Direct torque and flux control of induction machine using fuzzy logic controller," in *Proc. 2nd Int. Conf. Adv. Elect., Electron., Inf., Commun. Bio-Inform. (AEEICB)*, Chennai, India, Feb. 2016, pp. 193–197.

[24] Y. He, Y. Tang, D.-H. Lee, and J.-W. Ahn, "Suspending control method of BLSRM based on adaptive Fuzzy PID controller," in *Proc. IEEE Transp. Electrific. Conf. Expo, Asia–Pacific (ITEC Asia–Pacific)*, Busan, South Korea, Jun. 2016, pp. 755–760.

[25] X. Liu, B. Zhu, J. Zheng, and Z. Wang, "Air-gap-flux oriented optimized control of bearingless induction motor," in *Proc. 30th Chin. Control Conf.*, Jul. 2011, pp. 3549–3553.

[26] L. P. S. Junior, "Implementation of an intelligent radial position control system applied to an induction machine as divided winding-type drive motor," M.S. thesis, Federal Univ. Rio Grande do Norte, Natal, Brazil, 2017.

[27] S. Haffner, L. A. Pereira, and L. F. A. Pereira, "A method for optimization of five-phase induction machines based on genetic algorithms," *J. Control, Automat. Elect. Syst.*, vol. 26, no. 5, pp. 521–534, 2015.

[28] N. El Ouanjli, S. Motahhir, A. Derouich, A. El Ghzizal, A. Chebabhi, and M. Taoussi, "Improved DTC strategy of doubly fed induction motor using fuzzy logic controller," *Energy Rep.*, vol. 5, pp. 271–279, Nov. 2019.

[29] C. M. R. Osorio, J. L. A. Puma, D. B. Luque, J. A. T. A. Carcasi, and A. J. Sguarezi Filho, "Controle das potências do aerogerador de Indução com Rotor Bobinado com emprego de controladores PI e fuzzy tipo Mamdani," in *Proc. XII Simpósio Brasileiro de Automação Inteligente (XII SBAI)*, Santo André, Brazil, 2015.

[30] O. Oñederra, I. Kortabarria, I. M. de Alegría, J. Andreu, and J. I. Gárate, "Three-phase VSI optimal switching loss reduction using variable switching frequency," *IEEE Trans. Power Electron.*, vol. 32, no. 8, pp. 6570–6576, Aug. 2017.

EVANDRO AILSON DE FREITAS NUNES was born in Natal, Brazil. He is graduated in electric engineering from the Federal University of Rio Grande do Norte, the master's degree in electric engineering from the Federal University of Rio Grande do Norte, in 2017, and the Ph.D. degree in electric engineering, in 2018. He has been a Teacher with the Federal Institute of Bahia, IFBA, since 2018, where teaches contents of electrical systems analysis, electric machine drives, and electric machines theory. His current research interests include renewable energy generation, process automation, and the distribution of electric power.

ANDRÉS ORTIZ SALAZAR (M'11) was born in Lima, Peru. He is graduated in electronic engineering from the National University of Engineering, Lima, and the master's degree in electric engineering and the Ph.D. degree in electric engineering from the Federal University of Rio de Janeiro, Brazil, in 1989 and 1994, respectively. He held a postdoctoral position in electric engineering with the Tokyo University of Science, SUT, Japan, in 2000. He has been a Teacher with the Federal University of Rio Grande do Norte, since 1994, where teaches instrumentation, industrial automation, power electronics, machine activation, and automation. His current research interest includes the electronic automation of electrical and industrial processes.

ELMER ROLANDO LLANOS VILLARREAL (M'19) was born in Huánuco Peru. He received the B.Sc. degree in mathematics from the National University of Engineering, Lima, Peru, the master's degree in electric engineering from the Polytechnic School University of Sao Paulo, in 1997, and the Ph.D. degree in electric engineering from the Federal University of Santa Catarina, Brazil, in 2002. He held a postdoctoral position in electric engineering with the Federal University of Rio Grande do Norte, in 2019. He has been a Teacher with the Federal Rural University of Semi-arid, since 2009, where teaches linear algebra, linear systems, and numerical calculus. His current research interests include mathematical modeling and control systems.

FRANCISCO ELVIS CARVALHO SOUZA was born in Apodi Rio Grande do Norte, Brazil. He is graduated and received the master's and Ph.D. degrees in electric engineering from the Federal University of Rio Grande do Norte, in 2004, 2006, and 2011, respectively. He is currently a Professor with the Federal Institute of Education, Science and Technology of Rio Grande do (IFRN), Mossoró, Brazil. His research interests include electric machines, power electronics, power systems control, and nebulous logic applied to control.

LUCIANO PEREIRA DOS SANTOS JÚNIOR was born in Aracaju, Brazil. He is graduated in electric engineering by University Pio Decimo, in 2004, and received the master's and Ph.D. degrees in electric engineering from the Federal University of Rio Grande do Norte, in 2009 and 2017, respectively. He is currently a Professor with the Federal Institute of Education, Science and Technology of Rio Grande do Norte (IFRN), Natal, Brazil. His current research interests include electrical engineering, with emphasis on power electronics, working mainly in the following topics: three-phase PWM converters, PFCs, inverters, machines, microcontrollers, and processors applied in electronic power.

JOSÉ SOARES BATISTA LOPES was born in Natal, Brazil, in 1980. He received the B.S. degree in computing engineering from Potiguar University (UnP), Brazil, in 2004, and the M.Sc. and D.Sc. degrees in electrical engineering from the Federal University of Rio Grande do Norte (UFRN), in 2011 and 2016, respectively. He is currently a Professor with the Federal Institute of Education, Science, and Technology of Rio Grande do Norte Federal. His current research interests include automation, intelligent systems, and educational robots.

JUAN CARLOS CUTIPA LUQUE (M'15) was born in Arequipa, Peru. He is graduated in electronic engineering from the Universidad Nacional de San Agustin de Arequipa, Peru, in 2004, and the M.Sc. and Ph.D. degrees in mechanical engineering from the University of São Paulo, Brazil, in 2007 and 2012, respectively. He is currently a Professor with the Electronic Engineering Department, Universidad Nacional de San Agustin de Arequipa, Peru. His research interests include advanced control systems for autonomous underwater vehicles (AUVs), remote-operated submersible vehicles (ROVs), unmanned surface vehicles (USV), and electric vehicles.